https://doi.org/10.1070/RCR4960

Recent advances in computational liquid-phase ^{77}Se NMR

Leonid B. Krivdin [a, b]

[a] *A.E.Favorsky Irkutsk Institute of Chemistry, Siberian Branch of the Russian Academy of Sciences, ul. Favorskogo 1, 664033 Irkutsk, Russian Federation*
[b] *Angarsk State Technical University, ul. Tchaikovskogo 60, 665835 Angarsk, Irkutsk Region, Russian Federation*

This review aims to highlight significant progress in the calculation of ^{77}Se NMR chemical shifts and spin – spin coupling constants involving selenium substantiated with a vast amount of experimental data. The material is arranged in two basic sections: the first one dealing with the calculation of ^{77}Se NMR chemical shifts and the second one dealing with the computation of spin – spin coupling constants involving ^{77}Se nucleus, namely ^{77}Se – ^{1}H, ^{77}Se – ^{13}C and ^{77}Se – ^{77}Se together with some more exotic types of couplings, ^{77}Se – ^{15}N, ^{77}Se – ^{19}F, ^{77}Se – ^{29}Si and ^{77}Se – ^{31}P. A special attention is focused on the stereoelectronic effects involving selenium atom and their manifestation in the ^{77}Se NMR spectra of organoselenium compounds studied with the aid of the modern calculation of ^{77}Se NMR parametres in combination with experimental results.
The bibliography includes 114 references.

Contents

1. Introduction 266
2. Computation of ^{77}Se NMR chemical shifts 267
   2.1. Organoselenium compounds 267
   2.2. Transition metal complexes 271
3. Calculation of spin – spin coupling constants involving ^{77}Se nucleus 272
   3.1. ^{77}Se – ^{1}H spin – spin coupling constants 273
   3.2. ^{77}Se – ^{13}C spin – spin coupling constants 273
   3.3. ^{77}Se – ^{77}Se spin – spin coupling constants 275
   3.4. Other coupling constants involving ^{77}Se nucleus 276
4. Conclusion 277
   Abbreviations 277

Dedicated to Professor S.V.Amosova and Professor N.K.Gusarova (A.E.Favorsky Irkutsk Institute of Chemistry) in recognition of their valuable contribution to the field of organoselenium chemistry



Professor S.V.Amosova (left) and Professor N.K.Gusarova (right), Irkutsk (2013)

Professor Svetlana V. Amosova *graduated from Irkutsk State University in 1963 and received her PhD degree on the 'Reactions of sulfides and disulfides with acetylene' (Irkutsk, 1968) and her DSc degree on the 'New synthetic routes to organosulfur monomers and intermediates based on acetylene' (Irkutsk, 1979) and got her Full Professor in 1983 from the Irkutsk Institute of Organic Chemistry, Siberian Branch of the Russian Academy of Sciences. She was a Deputy Director of the title institute in the interim of 1986 – 2001. For many years she was a Deputy Chairman of the Scientific Council of the State Committee for Science and Technology leading the section of Synthetic and Theoretical Chemistry of Organic Sulfur Compounds. Svetlana Amosova was a scientific supervisor of 4 DSc and 21 PhD dissertations and the author of 1 book, 7 reviews, about 400 research papers and 250 patents.*

Under her supervision, a fundamental approach to the synthesis of organochalcogen compounds from chalcogen halides including selenium dichloride and dibromide was

Leonid Krivdin graduated from M.V.Lomonosov Moscow State University in 1977, received his PhD in 1982 from the Irkutsk State University, which was followed by a post-doctoral fellowship at Flinders University of South Australia in the group of Professor Ernst Della (1990 – 1991). He received his DSc in 1989 and Full Professor in 1993.
E-mail: krivdin_office@irioch.irk.ru
His research interests focus on computation of NMR parametres being substantiated with some 400 research publications including 15 reviews and book chapters. Under his scientific supervision, 12 PhD dissertations were defended in the interim of 1989 until present. He is currently a Head of the NMR Laboratory at the A.E.Favorsky Irkutsk Institute of Chemistry and a Chair of Chemistry at the Angarsk State Technical University.

Received 17 April 2020

© 2021 Uspekhi Khimii, ZIOC RAS, Russian Academy of Sciences and IOP Publishing Limited

developed. These new electrophilic reagents introduced for the first time in organic synthesis resulted in the implementation of a wide series of chemo-, regio- and stereoselective reactions to afford precursors of innovative highly efficient materials for micro- and nanoelectronics and potentially biologically active agents. The chemistry of divinyl chalcogenides and their analogues and derivatives, the unique building elements of organochalcogen compounds, intermediates and synthons of organic synthesis, was also developed under her supervision. As a result of her activity, a fundamental effect of anchimeric assistance of chalcogen atoms in new reactions and rearrangements was investigated and methods for the synthesis of the novel classes of unsaturated selenium-containing compounds possessing potential biological activity were developed. Novel methods for heterocyclization and annulation of chalcogen-containing heterocyclic systems using selenium dihalides via the sigmatropic rearrangements were carried out under her guide to produce new conducting materials and biologically active compounds.

Svetlana Amosova developed the unique methods for the preparation of important polyunsaturated hydrocarbons via the cross-coupling of acetylene and its derivatives with halogen-containing compounds using inexpensive palladium-free catalysts. In the course of this study, the novel regio- and stereoselective fundamental approaches to practically important chalcogen-containing compounds were suggested. Those methods involved generation of highly reactive nucleophilic reagents from elemental chalcogens or organic diselenides together with their introduction to nucleophilic addition and substitution reactions. Also, the novel organochalcogen-based drugs were discovered in her laboratory. As an example, the highly effective antituberculosis drug Perkhlozon was introduced into clinical practice. As a result, a direct synthesis of the analogues and derivatives of Perkhlozon, Ebselen and AS-101, was implemented in the design of new biologically active compounds.

***Professor Nina K. Gusarova** graduated from Irkutsk State University in 1965 and received her PhD degree on the 'Reaction of organic disulfides with acetylenes' (Irkutsk, 1971) and her DSc degree on the 'Reactions of chalcogenes with acetylenes — new routes to α,β-unsaturated sulfides, selenides and tellurides' (Irkutsk, 1986) and got her Full Professor in 1997 from the Irkutsk Institute of Organic Chemistry, Siberian Branch of the Russian Academy of Sciences. In 2014, she became an Honored Scientist of the Russian Federation. She is a well-known specialist in organic chemistry of sulfur, selenium and tellurium and is mostly known for the development of the construction of α,β-unsaturated chalcogenides based on the one-pot synthesis of chalcogenides with acetylenes in the superbase media. These studies were repeatedly supported through the grants of the Russian Fundation for Basic Research and the Russian Science Fundation and substantiated through the cooperation with universities and private companies of Netherlands, Germany and South Korea. She is a Laureate of the Russian Presidential and Government Scholarship for Russian Presidential and Government Scholarship for leading scientists of Russia and the editorial board member of the Arkivoc journal. Nina Gusarova was a scientific supervisor of 2 DSc and 16 PhD dissertations and the author of 3 books, 19 reviews, more than 450 research papers and about 100 patents.*

Nina Gusarova is known for the investigation of the new multicomponent reactions between primary or secondary phosphines, elemental chalcogens and organic and inorganic bases. She applied a new strategy for the one-pot atom-economic synthesis of chalcogene phosphinic and chalcogene phosphonic acid derivatives, highly effective precursors for the design of semiconductor, optical and magneto-optical nanomaterials, new generation pesticides. As a result, a number of highly selective extraction reagents for the fractionation of rare, precious and radioactive metals were developed in the course of these studies. Per group was the first to show that zwitterionic vinyl carbanions, formed upon the attack of tripyridylphosphine on electron-deficient acetylenes, trigger a new stereoselective synthesis of the unknown functionalized vinyldipyridylphosphine oxides. This reaction proceeds in water without catalyst under slight heating with C—P bond cleavage and pyridine abstraction. Isomerically pure vinyldipyridylphosphine oxides are promising ligands for metal complex catalysts, drug precursors and intermediates in the organic synthesis.

As another perspective implementation of her activity in organic synthesis, Nina Gusarova with her collaborators carried out a straightforward synthesis of diselenophosphinic acid esters directly from elemental phosphorus, selenium and alkenes in two preparative stages. The first stage involved chlorine-free environmentally safe direct phosphorylation of alkenes by elemental phosphorus in a superbase system to deliver secondary phosphines. The second stage comprised a new three-component, atom-economic, regioselective reaction between secondary phosphines, elemental selenium and alkenes. This profound reaction proceeds under mild conditions without catalyst to furnish an unknown class of organophosphoselenium compounds, containing chiral carbon at the selenium atom. Derivatives of the synthesized diselenophosphinates are employed for the preparation of the semiconductor nanomaterials, nano-structured selenium and represent polymerization regulators (known as RAFT agents) and a variety of other biologically active compounds.

P.S. This photo was taken by the author in 2013 during the 27th International Conference 'Chemical Reagents and Processes of Small Tonnage Chemistry' (Irkutsk, 21–24 October, 2013).

1. Introduction

Significant progress in theoretical NMR spectroscopy [1] and, in particular, in the NMR-oriented calculations,[2–8] involving those at a relativistic level,[9–12] for the most common 1/2 spin NMR isotopes of the first three periods — proton,[13–15] carbon,[16–18] nitrogen,[19] fluorine,[20] silicon,[21] and phosphorus,[22,23] is rapidly developing and becoming of more and more practical interest. In this line, in view of the substantial progress in the calculation of ^{77}Se NMR chemical shifts and spin–spin coupling constants involving ^{77}Se nucleus[24,25] substantiated with a vast amount of available experimental data, the review of the computational aspects of ^{77}Se NMR appears to be timely and being on the cutting edge of modern computational chemistry. The data are arranged in two basic sections — the first one dealing with the calculation of ^{77}Se NMR chemical shifts (Section 2) and the second one dealing with the computation of spin–spin coupling constants involving ^{77}Se nucleus, namely ^{77}Se—^{1}H, ^{77}Se—^{13}C and ^{77}Se—^{77}Se (Section 3). Additionally, some more exotic types of couplings, ^{77}Se—^{15}N, ^{77}Se—^{19}F, ^{77}Se—^{29}Si and ^{77}Se—^{31}P, are also briefly reviewed in Section 4. A special attention is focused on stereoelectronic effects involving selenium atom and their applications based on the calculations of the ^{77}Se NMR parametres.

Based on the selenium position Periodic Table, one should expect the manifestation of relativistic effects in both selenium chemical shifts and selenium spin–spin coupling constants, as compared, for example, to carbon NMR parametres. In general, relativistic effects in the values of NMR parametres include electron spin–orbit coupling (the interaction of the spin magnetic moment of an electron with the magnetic field induced by its own orbital motion) and scalar effects, the so-called Darwin term (relativistic fluctuation of an electron about its mean position) and mass-velocity corrections (relativistic increase in the mass of an electron with its velocity approaching the speed of light). This strongly affects the NMR shielding constants of heavy nuclei and, on the other hand, light nuclei in heavy environment. Accordingly, there are two most significant types of relativistic effects, namely the so-called scalar effects, *i.e.* the ones operators of which do not contain the electronic spin variable, and, on the other hand, spin-orbit relativistic effects, *i.e.* those operators of which depend on the electronic spin. Both two types of relativistic effects in the ^{77}Se NMR chemical shifts and selenium spin–spin coupling constants are thoroughly discussed in different sections of the present review.

The second peculiarity of the selenium atom is the presence of the hybridized lone pair capable of different intramolecular interactions with the neighboring molecular orbitals and molecular moieties providing a variety of stereochemical effects in the selenium NMR parametres. This issue is also comprehensively covered in the present review substantiated with a number of illustrative examples.

Basically, this review is intended for NMR spectroscopists and synthetic chemists, utilizing modern computational methods in their everyday scientific activity for the calculation and interpretation of ^{77}Se NMR spectra of a vast amount of organoselenium compounds.

2. Computation of ^{77}Se NMR chemical shifts

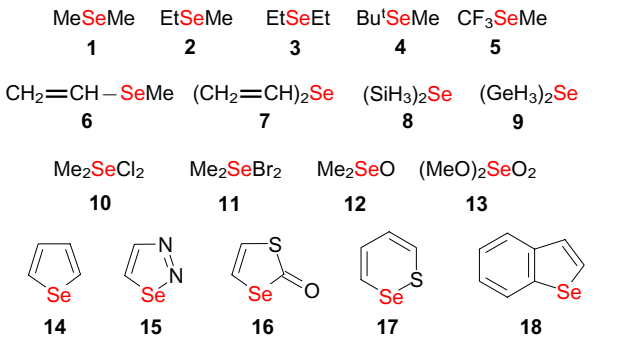
Herewith, we will not go back in history deeper than 2010, only paying tribute to the most prominent (in our opinion) early papers on computational ^{77}Se NMR presented in the most essential publications by a number of different authors.[26–44] This Section begins with the discussion of the most representative recent calculations of ^{77}Se NMR chemical shifts performed in the series of the simplest and larger medium-sized organoselenium compounds passing afterwards to the selenium containing transition metal complexes.

2.1. Organoselenium compounds

Starting this section with the reviewing of the computational ^{77}Se NMR of small organoselenium compounds, it should be recalled that in two related papers by Rusakov *et al.*,[45,46] the ^{77}Se NMR chemical shifts were calculated in the series of a couple of dozens of the most representative organoselenium compounds **1**–**18** in terms of a full four-component DFT and relativistic random phase approximation (RPA).

Among six functionals (B3LYP, KT2, KT3, LDA, PBE and PBE0) tested in the first paper[45] at a four-component level in combination with relativistic Dyall's basis set, dyall.av3z, best result was achieved with the NMR-oriented Keal–Tozer KT2 functional characterized by an unprecedentedly small MAE of 30 ppm for the span of ^{77}Se NMR chemical shifts of as much as about 1700 ppm, as illustrated in Fig. 1.

Structures 1–18



It is noteworthy that according to the results of the second paper,[46] almost all DFT methods performed noticeably better than RPA which was due to the fact that correlation effects were of major importance in the reproduction of experimental ^{77}Se NMR chemical shifts. As a result, the uncorrelated RPA method, not taking into account correlation effects, demonstrated noticeably worse performance, as compared to almost all DFT functionals (Fig. 2). Another finding of the performed study[46] was that the influence of the relativistic geometrical effects on calculated ^{77}Se NMR chemical shifts was surprisingly insignificant, almost next to negligible (1–2 ppm), so that relativistic effects could safely be neglected in most cases. However, for molecules containing 'heavy' elements starting with the fourth period in the selenium environment, the usage of relativistic geometries was strongly recommended. Solvent corrections to the ^{77}Se NMR chemical shifts were found to be far from negligible falling into range of about 10–30 ppm reaching for some compounds as much as about 50–60 ppm.

Another interesting finding of the performed calculations[46] was that vibrational and solvent corrections essentially compensated each other, so that one factor should not be ignored when taking into account another one. This is

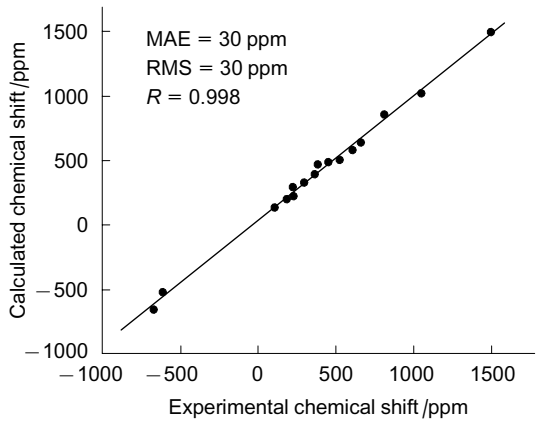


Figure 1. Correlation plot of ^{77}Se NMR chemical shifts in the series of **1**–**18** calculated at the GIAO-4DFT-KT2/dyall.av3z level using relativistic geometries and taking into account solvent effects *vs.* experiment (best results). *R* is Pearson correlation coefficient. Reproduced from Rusakov *et al.*[45] with the permission of *John Wiley and Sons*.

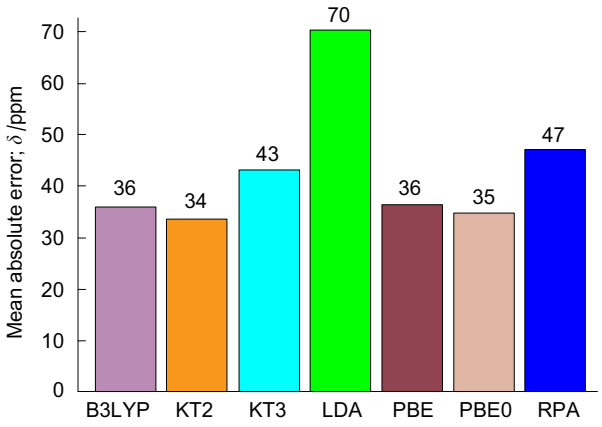


Figure 2. Mean absolute errors (ppm) of ^{77}Se NMR chemical shifts of **1**–**18** calculated using different functionals at the four-component DFT level, as benchmarked to the RPA results *vs.* experiment. Used acronyms and abbreviations: B3LYP is the Becke three-parametre hybrid functional in combination with the Lee–Yang–Parr correlation functional, KT2 is the generalized gradient exchange-correlation functional of Keal and Tozer, KT3 is the generalized gradient exchange-correlation functional of Keal and Tozer with the gradient-corrected exchange and correlation terms, LDA is the local density approximation, PBE is the Perdew–Burke–Ernzerhof generalized gradient functional, PBE is the Perdew–Burke–Ernzerhof generalized gradient functional with a predetermined amount of exact exchange and RPA is the random phase approximation. Reproduced from Rusakov *et al.*[46] with the permission of *John Wiley and Sons*.

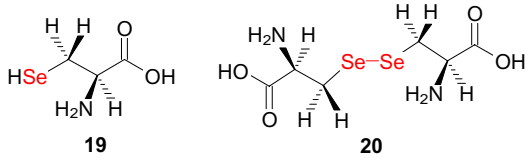
illustrated in Table 1 providing the results supporting this recommendation. It was also found that relativistic geometrical corrections were next to negligible. Taking into account all mentioned corrections, evaluated at the DFT level, resulted in an unprecedentedly accurate agreement between the performed SOPPA(CC2) calculations and experiment, as exemplified in Table 1.

In continuation of the earlier studies,[47–50] Zhang and co-workers[51] performed a detailed investigation of the effects of protonation, medium and substituent at the selenium-bonded carbon on isotropic ^{77}Se NMR chemical shifts of the genetically encoded amino acid selenocysteine (**19**) and its dimeric form, selenocystine (**20**). These effects were monitored by experimental and calculated ^{77}Se NMR chemical shifts. Indeed, these studies essentially contributed to the understanding of the nature of a diselenide bond. The conformational effect was found to spread to as much as *ca.* 600 ppm for the C–Se–Se–C dihedral angle ranging from −180 to +180°. As a result, ^{77}Se NMR chemical shifts were

Table 1. Corrections to ^{77}Se NMR chemical shifts (ppm), calculated at the four-component relativistic GIAO-4DFT-KT2 level. Compiled from Rusakov *et al.*[46]

Compound	Uncorrected value	Corrections			Total	Experiment
		vibrational	solvent	geometrical		
8	−680	−28	20	−6	−692	−666
10	436	−32	50	4	458	449
12	813	−26	42	2	830	812
14	561	−15	23	−1	567	613
15	1444	−16	47	5	1476	1502
17	206	−10	20	1	216	228

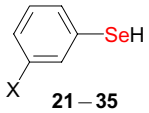
Structures 19, 20



found to be a sensitive probe to such changes having a chemical shift range of about 270 ppm.

Several years ago Sladek *et al.*[52] performed the B3LYP/6-311++G(d,p) calculations of the isotropic ^{77}Se NMR chemical shifts in gas phase (*i.e.* with no solvent effect taken into account) for a series of fourteen *m*-substituted selenophenols **21**–**35**. The main idea of this publication (as far, as it might be understood by the reader) was to find a solid correlation between ^{77}Se NMR chemical shifts and Hammett's sigma constants. However, no such correlations were found for selenium chemical shifts. Unfortunately, no relativistic effect of 'heavy' bromine on the ^{77}Se NMR chemical shift in compound **35** was either taken into account or discussed in any way.

Structures 21–35

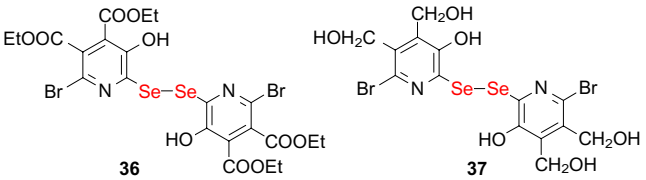


X = H (**21**), Me (**22**), CF_3 (**23**), COMe (**24**), CO_2Me (**25**), CO_2Et (**26**), CN (**27**), OH (**28**), OMe (**29**), O–Pr^i (**30**), NH_2, (**31**) SH (**32**), F (**33**), Cl (**34**) and Br (**35**)

In search for the structural modifications of the vitamin B6 scaffold together with the related glutathione peroxidase, which serve as cofactors in the metabolism of amino acids, performed by Singh and co-workers,[53–57] pyridoxine-like diselenides **36** and **37** were prepared and thoroughly investigated by means of experimental and computational ^{77}Se NMR.[58] Based on the ^{77}Se NMR experiments, substantiated by the calculation of ^{77}Se NMR chemical shifts, a catalytic mechanism for diselenide **36** was proposed, which involved selenol, selenosulfide and seleninic acid intermediates. It was shown that the bromine substituent increased a positive charge on selenium, which was confirmed by the natural population analysis (NPA) and observed in the calculated and experimental ^{77}Se NMR chemical shifts.

Also, it was shown[58] that the dipyridyl diselenide moiety was kept in an almost planar *transoidal* conformation. According to the natural bond orbital (NBO) analysis, this was due to the weak intramolecular Se···O and Se···N interactions. The effect of bromine was found in the calculated as well as in the experimental ^{77}Se NMR chemical shifts. The ^{77}Se NMR chemical shifts of **36** and **37** were calculated in gas phase at the B3LYP/6-311+G(d,p) level on the B3LYP/6-31+G(d) geometries giving 598 ppm for

Structures 36, 37

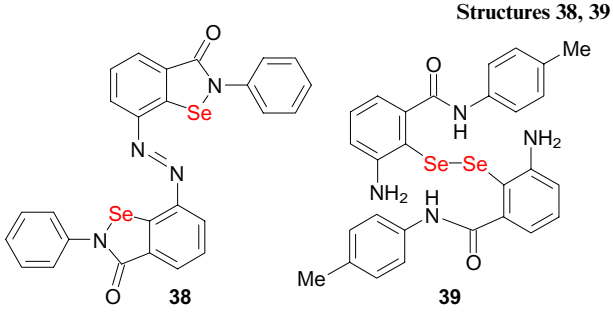


36 and 563 ppm for **37** from Me_2Se (experimental values were accordingly, 450 and 408 ppm). No relativistic effect of heavy bromine was expected in the ^{77}Se NMR chemical shifts separated by as many as four chemical bonds, so that no relativistic corrections were needed at either two- or four-component levels for these particular systems.

In the forthcoming paper by the same principal authors,[59] novel azo-bis-ebselen **38** was prepared, which was shown to be completely planar, and this was explained to be due to the strong intramolecular Se···N interactions. The later were found to be much stronger than the corresponding Se···O interactions in related nitroebselens.

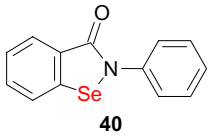
Based on experimental and computational ^{77}Se NMR spectroscopy, a catalytic cycle for diselenide **39** was proposed in the same paper.[59] To find out more about the effect of the intramolecular secondary Se···N/O interactions on chemical bonding and the ^{77}Se NMR chemical shifts, extensive DFT calculations were carried out. The magnitudes of the $n_N \rightarrow \sigma^*_{SeN}$ and $n_O \rightarrow \sigma^*_{SeN}$ orbital interactions suggested a significant covalent interaction between the nitrogen lone pair and the low-lying antibonding orbital of the selenium atom. Interesting to note, the performed NBO analysis indicated that the Se···N interactions were much stronger than the corresponding Se···O interactions. Calculated ^{77}Se NMR chemical shifts were in a good agreement with the experimental values supporting this finding.

Structures 38, 39



Zielińska-Błajet and co-workers[60] performed extensive DFT calculations of the ^{77}Se NMR chemical shifts for the lowest energy conformers of the derivatives of ebselen, 2-phenyl-1,2-benzisoselenazol-3(2*H*)-one (**40**), a promising antioxidant and antiinflammatory agent, also known as an oxygen and bromine transfer catalyst.

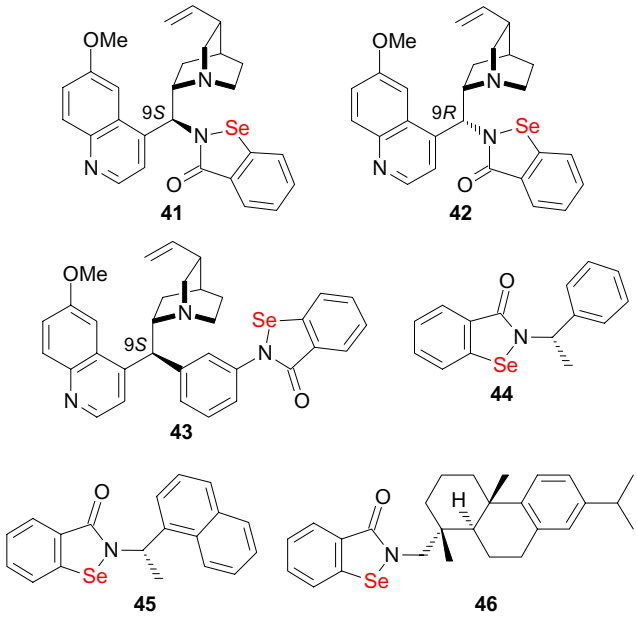
Structure 40



In this paper,[60] six 1,2-benzisoselenazol-3(2*H*)-ones (**41**–**46**) were synthesized and carefully studied by means of theoretical calculations of their ^{77}Se NMR chemical shifts at the DFT level using the B97-2 hybrid functional (Becke's B-97 functional[61] reparameterized by Wilson *et al.*[62]) and Dunning's cc-pVTZ basis set. Calculated ^{77}Se NMR chemical shifts for the lowest energy conformers of **41**–**46** (with their stereochemical structures shown in Fig. 3) are given in Table 2. It was found that they were in a fairly good agreement with experimental data, while the conformers of higher energy provided markedly worse fit.

Not surprisingly, B97-2 results reproduced the experiment much better, as compared to the B3LYP calculations. In those calculations, the DFT isotropic shieldings were scaled to the experimental chemical shifts assuming the ^{77}Se

Structures 41–46



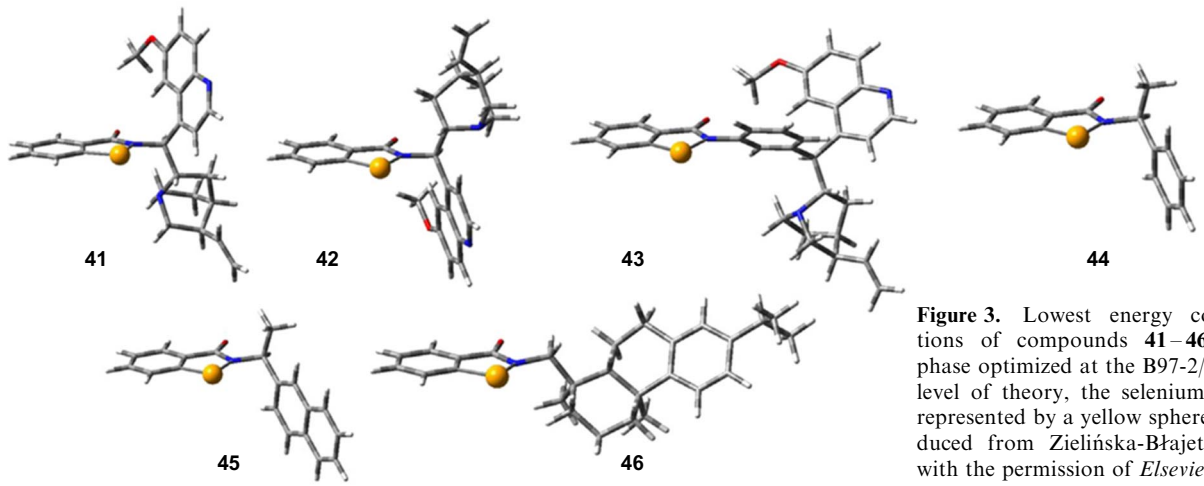


Figure 3. Lowest energy conformations of compounds **41**–**46** in gas phase optimized at the B97-2/cc-pVTZ level of theory, the selenium atom is represented by a yellow sphere. Reproduced from Zielińska-Błajet *et al.*[60] with the permission of *Elsevier*.

Table 2. Scaled ^{77}Se NMR chemical shifts (ppm) calculated at the DFT level, as compared to experiment ($CDCl_3$). Compiled from Zielińska-Błajet *et al.*[60]

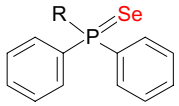
Compound	B3LYP	B97-2	Experiment
41	824.8	853.0	860.8
42	830.5	869.7	859.2
43	966.6	968.8	947.8
44	804.5	835.3	830.4
45	813.4	841.1	844.6
46	913.3	935.6	932.8

NMR chemical shifts of accordingly, 0 and 960 ppm for dimethyl selenide and ebselen. Additionally, for compounds **41**–**43** protonated at the nitrogen atom of the quinuclidine ring, the magnetic shieldings were calculated at the same level of theory. As a result, in compound **41**, a significant change of the geometry on protonation was predicted, and an additional proton was expected to participate in the hydrogen bonding with the carbonyl of the isoselenazolone moiety. This change was manifested in a marked increase (176 ppm) in the calculated ^{77}Se NMR chemical shift.

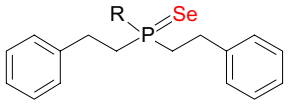
At the same period of time, Chernyshev *et al.*[63] performed the two-component relativistic ZORA-B1PW91/TZP calculations of the ^{77}Se NMR chemical shifts in the series of phosphine chalcogenides **47**–**54**, as illustrated in Table 3. It was found that the effect of the conformation related to the internal rotation about the single P–C bonds was insignificant, and the contribution of the relativistic spin–orbit term to the ^{77}Se NMR chemical shifts did not exceed 10 ppm.

In continuation of the earlier studies by the teams of Nolan and Covallo,[64–72] an interesting result was reported[73] dealing with the computational studies of selenoureas **55**–**78** shown in Fig. 4. In the course of this study, an interconnection was established between the shielding of

Structures 47–54



47–49



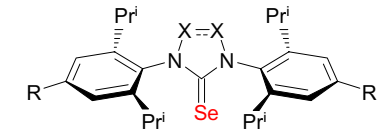
50–54

R = H (**47**, **50**), Pr_2N (**48**), PhCH=CH (**49**, **54**) Me (**51**), Me_2N (**52**), MeO (**53**)

Table 3. ^{77}Se NMR chemical shifts (ppm) of phosphine chalcogenides, calculated at the ZORA-B1PW91/TZP level, as compared to experiment ($CDCl_3$). Compiled from Chernyshev *et al.*[63]

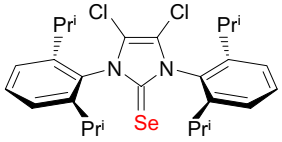
Compound	Non-relativistic	Spin–orbit contribution	Relativistic	Experiment
47	–396.9	–10.3	–407.2	–
48	–364.8	–6.0	–370.8	–277.7
49 (*E*)	–280.9	–11.7	–292.6	–
49 (*Z*)	–255.2	–11.0	–266.2	–
50	–461.7	–6.7	–468.4	–413.9
51	–389.4	–6.4	–395.8	–341.6
52	–370.3	–7.6	–377.9	–308.1
53	–341.9	–5.4	–347.3	–345.3
54 (*E*)	–276.6	–6.9	–283.5	–
54 (*Z*)	–215.8	–10.7	–226.5	–

the selenium centre and electronic properties of N-heterocyclic carbenes (known in the literature as 'NHC'). These results showed that selenium chemical shifts are well correlated with the energy gap between an occupied lone pair orbital on selenium and vacant π* orbital corresponding to the Se–NHC bond. On the other hand, bond energy decomposition analysis indicated no correlation between the sigma-orbital contribution to the ^{77}Se NMR chemical shifts, while a good correlation was found between the

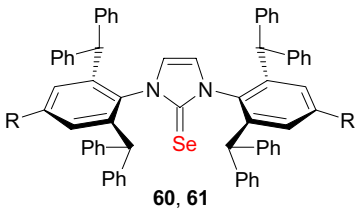


55–58

X = CH, R = H (**55**); X = CH, R = OMe (**56**); X = CH_2, R = H (**57**); X = CH_2, R = OMe (**58**)

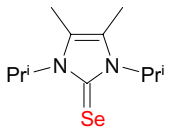


59

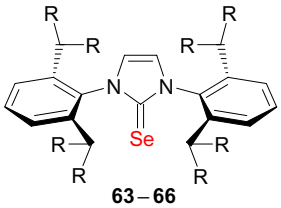


60, **61**

R = Me (**60**), OMe (**61**)

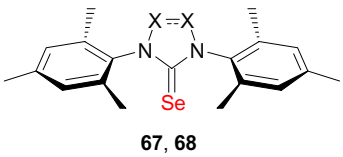


62



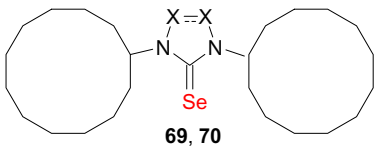
63–66

R = H (**63**), Et (**64**), Pr^n (**65**), Bu^n (**66**)



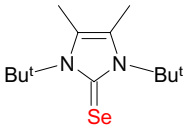
67, **68**

X = CH (**67**), CH_2 (**68**)

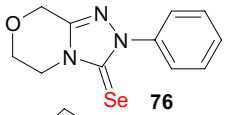


69, **70**

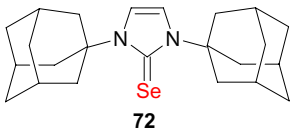
X = CH (**69**), CH_2 (**70**)



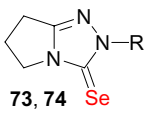
71



76

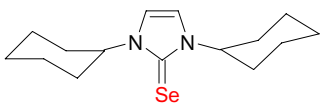


72

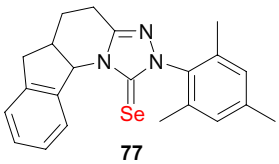


73, **74**

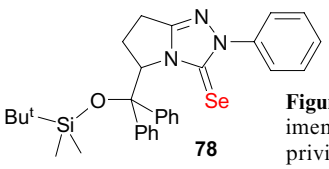
R = Mes (**73**), C_6F_5 (**74**)



75



77



78

Figure 4. A set of representative selenourea compounds studied by experimental and computational ^{77}Se NMR. Reproduced with minor editing privilege from Vummaleti *et al.*[73] with the permission of *The Royal Society of Chemistry*.

π-contribution to the selenium chemical shielding in that series. More detailed analysis of the selenium paramagnetic shielding in terms of molecular orbitals indicated that $\sigma_p(xx)$ depend mainly on the $Se(p_y) \rightarrow Se-NHC(\pi^*)$ transitions between the occupied p_y orbital on the selenium atom and the virtual π* orbital of selenourea. For all of the 24 studied selenoureas, the ^{77}Se NMR shieldings derived from the performed calculations correlated with those obtained experimentally. Also, all of the calculated ^{77}Se NMR shieldings were found to be strongly correlated with the $Se(p_y) \rightarrow Se-NHC(\pi^*)$ energy gap and the charge at the selenium centre.

In the paper by Liske *et al*,[74] a new method for the assessment of the π-acceptor strength of *N*-heterocyclic carbenes was presented. The ^{77}Se NMR chemical shifts of selenium carbene adducts correlated well with the π-acceptor character of the respective carbenes. The observed ^{77}Se NMR chemical shifts covered a wide range of almost 800 ppm, with increasing π-acidity leading to a downfield shift of the selenium signal.

Two years later, Verlinden *et al.*[75] studied electronic properties of *N*-heterocyclic carbenes using the ^{77}Se NMR chemical shifts of their NHC–Se adducts to evaluate the π-acceptor properties. It was found that $^1J_{Se,C}$ spin–spin coupling constants provide insight into the σ-donor ability of the respective carbine, which was also supported by the DFT calculations.

2.2. Transition metal complexes

A number of selenium-containing complexes of transition metals have been extensively investigated in a series of recent publications by Brennan and co-workers [76–87] and also by Laitenen and co-workers,[88–97] where ^{77}Se NMR chemical shifts were computed at a high level of theory.

Thus, in one of the most recent and representative papers [85] from the group of Brennan, a series of selenium-containing thorium cubanes of the general formula $(py)_8Th_4(\mu3\text{-}E')_4(\mu2\text{-}EPh)_4(\eta\text{-}EPh)_4$ (E, E′ = S, Se) were prepared by the redox reactions of elemental sulfur and selenium with $Th(SPh)_4$ and $Th(SePh)_4$, exemplified by the structure of $(py)_8Th_4(\mu3\text{-}Se)_4(\mu2\text{-}SePh)_4(\eta\text{-}SePh)_4$ shown in Fig. 5. The computational analysis of their ^{77}Se NMR chemical shifts provided insight into the solution structure of these clusters.

In these calculations, all-electron relativistic DFT computation of the ^{77}Se NMR shielding constants was performed with the PBE0 exchange correlation functional with a 40% exact-exchange admixture (PBE0-40HF) in combination with the triple-zeta doubly polarized basis set (TZ2P) for thorium, selenium and sulfur atoms and double-zeta polarized basis set (DZP) of Slater-type orbitals for the lighter ligand atoms (C, H, N, F). Both scalar and spin-orbit relativistic effects were treated in terms of the ZORA formalism, while bulk solvent effects were simulated within the COSMO scheme. Computed ^{77}Se nuclear shielding constants were converted into chemical shifts relative to the shielding of Me_2Se, calculated at the same level of theory (functional, basis set). An excellent match between experimental and the DFT-computed ^{77}Se NMR shifts for pyridine-coordinated thorium cubanes supported the existence of the tetrametallic Th_4Se_4 structures coordinated by two pyridine molecules at each thorium centre in solution. No exchange between bridging and terminal SePh sites on the NMR time scale was found.

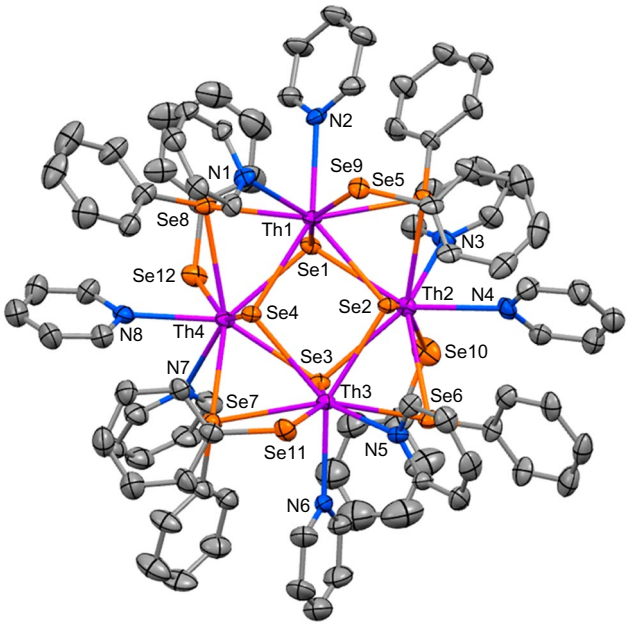


Figure 5. Thermal ellipsoid diagram of $(py)_8Th_4(\mu3\text{-}Se)_4(\mu2\text{-}SePh)_4(\eta\text{-}SePh)_4$ with the hydrogen atoms removed for clarity and ellipsoids at the 50% probability level. Reproduced from Ringgold *et al.*[85] with the permission of the *American Chemical Society*.

In another representative publication [79] from this group, a spherical cluster $(py)_{16}Ln_{17}NaSe_{18}(SePh)_{16}$ shown in Fig. 6 was reported. In these cluster, all three elements, lanthanum (Ln), sodium (Na) and selenium (Se), formed isostructural moieties with the molecular structure containing the central Ln ion surrounded by eight five-coordinate Se^{2-} ions enclosed in a group of sixteen lanthanum atoms. It was shown, both synthetically and computationally, that the presence of the Na^+ cation was a key factor to the formation of such clusters.

In the paper by Wu *et al.*,[87] an analysis of computational and experimental ^{77}Se NMR chemical shifts revealed that solvated dimeric structures with two bridging dichalcoge-

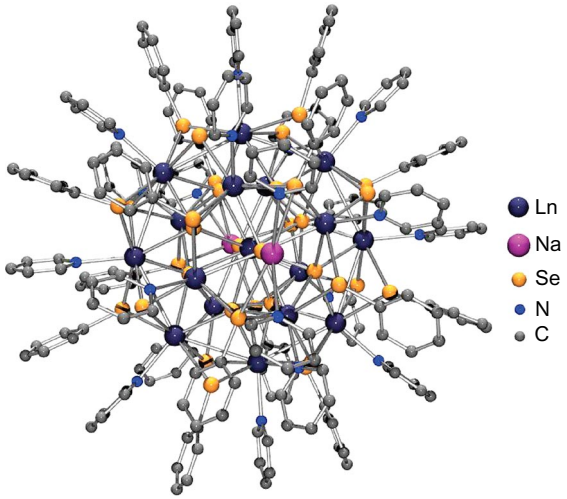


Figure 6. An ORTEP diagram of $(py)_{16}Ln_{17}NaSe_{18}(SePh)_{16}$ in the crystal with the hydrogen atoms removed for clarity. Reproduced from Moore *et al.*[79] with the permission of the *American Chemical Society*.

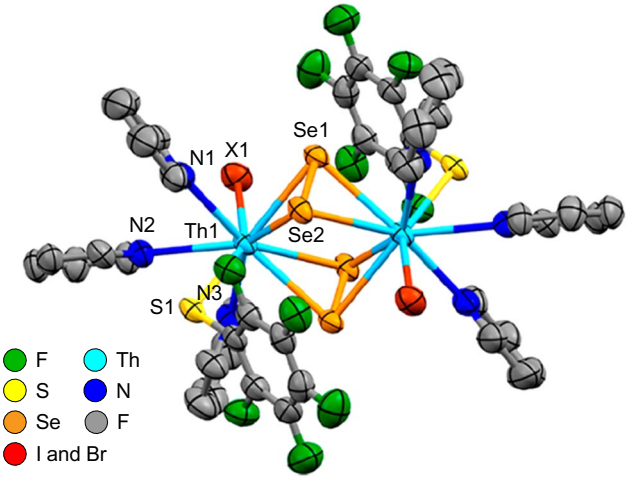


Figure 7. An ORTEP diagram of $(py)_6Th_2X_2(SC_6F_5)_2(Se_2)_2$, where X = I (**79**) and Br (**80**). Hydrogen atoms are removed for clarity, and ellipsoids are at the 50% probability level. Reproduced from Wu *et al.*[87] with the permission of the *American Chemical Society*.

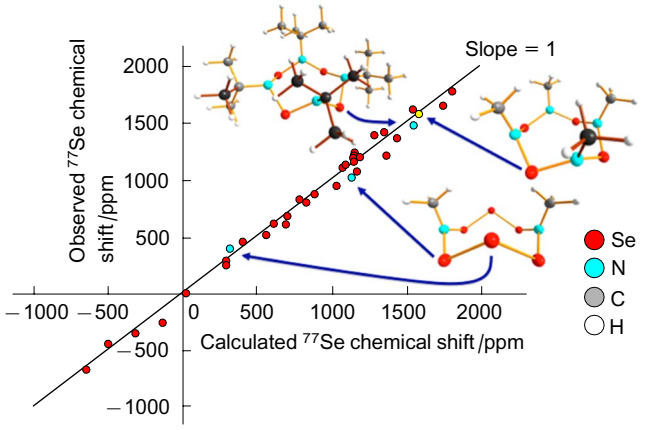


Figure 8. Correlation between the observed and PBE0/def2-TZVPP-computed ^{77}Se NMR chemical shifts of the selenium-containing prospective ligands. The red points represent molecules, for which experimental ^{77}Se NMR chemical shifts are unambiguously known, while blue and yellow ones are represented with chemical structures shown in an explicit way. Reproduced from Karhu *et al.*[90] with the permission of the *American Chemical Society*.

nides, exemplified by complexes **79** and **80** shown in Fig. 7, were present in solution. Chemical shift calculations were performed using the hybrid PBE0-40HF functional at the two-component ZORA relativistic level, including spin-orbit coupling. The investigated complexes were fully optimized at the DFT-PBE0/ECP/def2-TZVP level using the quasi-relativistic small-core pseudopotentials for heavy thorium and iodine, along with atom-pairwise dispersion corrections.

Experimental ^{77}Se NMR shifts of complexes **79** and **80** showed single ^{77}Se NMR resonances at 332 and 309 ppm, respectively, in a very good agreement with the performed calculations (328 and 318 ppm), all in the range expected for diselenides bridging two Th(IV) ions. Thus, experimentally observed ^{77}Se NMR shifts for pyridine-d_5 solutions of complexes **79** and **80** matched very well with the DFT computed values and were consistent with the dimeric structures of these complexes in solution. Not surprisingly, the desolvated species (those with no pyridine ligands attached to thorium) were shown to be absent in solution, and these hypothetical molecules were computed to be deshielded by about as much as 200 ppm relative to their solvated species.

Replacing the iodide ligands with their lighter analogues (Br^-, Cl^-) leads to the slightly longer Th–Se distances that were also reflected in small but noticeable upfield ^{77}Se NMR shifts, which was also evident from the experimental data for the title complexes **79** and **80**, in good agreement with the performed calculations. This was rationalized Wu *et al.*[87] to be a consequence of the stronger π-donating abilities in the series of $I^- < Br^- < Cl^-$, which in turn weakened the Th–Se bond covalency in mixed Th chalcogenide-halide complexes on going up the halogen group.

Among the publications by the group of Laitenen, one of the most representative paper was that by Karhu *et al.*[90] reporting the shielding tensors of 28 selenium-containing compounds, for which ^{77}Se NMR chemical shifts were calculated at the PBE0/def2-TZVPP level of theory. A spectral assignment in a series of new cyclic selenium imides, the prospective ligands of transition metal complexes, was performed based on these calculations. A good agreement between calculated and experimental values of ^{77}Se NMR chemical shifts was achieved, as illustrated in Fig. 8, and a good performance of the PBE0 functional in the prediction of the selenium magnetic properties was thus documented.

The mean deviation between the calculated and experimental ^{77}Se NMR chemical shifts achieved by Karhu *et al.*[90] was as small as 46 ppm for 32 different chemical shifts of 28 reference molecules. This is somewhat 10–30 ppm smaller than the corresponding the selenium chemical shifts obtained at the DFT (BP86), HF and MP2 levels of theory in the earlier publications.[98, 99]

It is well known that the effect of different solvents on ^{77}Se NMR chemical shifts is about 20–30 ppm. Thus, it followed that computations of the selenium chemical shifts, which were performed by Karhu *et al.*[90] for the individual molecules in vacuum, were close to the limit of accuracy that can be achieved for the molecules in solution. More precise calculations can be obtained by taking into account solvent and relativistic (not to say about the rovibrational) effects. The reported results of the performed calculations were found to be in a fairly good agreement with the available experimental data. In general, the suggested approach to use optimized geometries and calculated shielding tensors in gas phase, as compared to experimental data in solution, represented a reasonable compromise between precision and computational cost.

3. Calculation of spin–spin coupling constants involving ^{77}Se nucleus

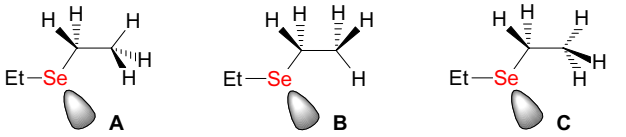
Calculations of spin–spin coupling constants involving selenium are much less common, as compared to those of ^{77}Se NMR chemical shifts. Herewith, we will focus briefly on the most significant recent papers dealing with the calculation of spin–spin coupling constants involving selenium, mainly ^{77}Se–^{1}H, ^{77}Se–^{13}C and ^{77}Se–^{77}Se, which were already partly reviewed by Rusakova and Krivdin[24] and Krivdin and Rusakov,[25] together with some more exotic types of couplings, namely ^{77}Se–^{15}N, ^{77}Se–^{19}F, ^{77}Se–^{29}Si and ^{77}Se–^{31}P.

3.1. ^{77}Se–^{1}H spin–spin coupling constants

Theoretical calculations this type of coupling constants are presented in the literature mostly by a series of publications from one group,[100–109] which are already reviewed by the principal authors.[24, 25]

As an example of these studies, Rusakov and Krivdin [108] performed a theoretical investigation of geminal and vicinal selenium–hydrogen coupling constants in two benchmark compounds — dimethyl and diethyl selenides at the most sophisticated SOPPA level to reveal their stereochemical behaviour with respect to the three main structural factors, namely, (i) the dihedral angle dependences; (ii) the bond angle dependences and (iii) the lone pair effects. It was demonstrated that both geminal and vicinal couplings provided a unique stereospecificity with respect to these factors, which was evidenced by a $^{3}J_{Se,H}$ dihedral angle dependence of the internal rotations about the carbon–carbon and carbon–selenium bonds in diethyl selenide, as illustrated in Fig. 9. The conformations **A**, **B** and **C** depicted in this figure are shown below. The dihedral angle dependences of geminal and vicinal selenium–hydrogen coupling constants, which were established by Rusakov and Krivdin,[108] were found to be of prime importance for the stereochemical studies of a wide range of organoselenium compounds.

Structures A–C



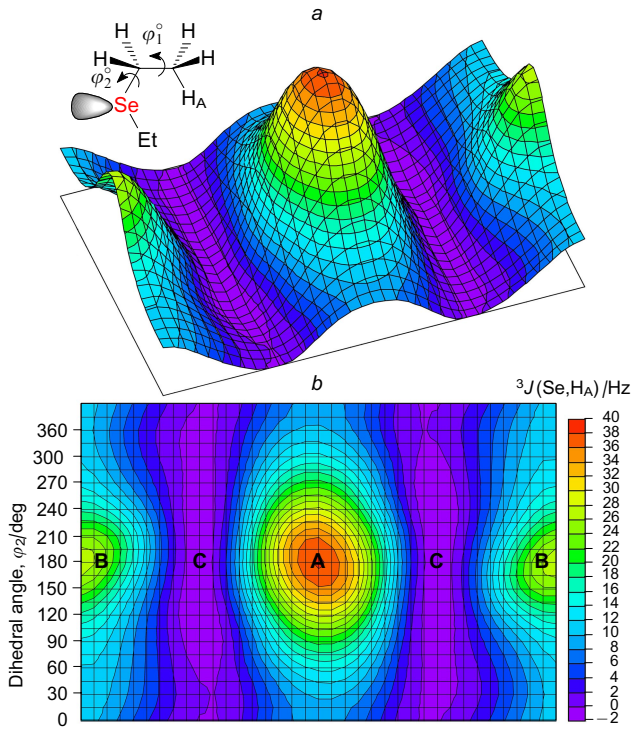
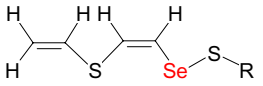


Figure 9. Spin–spin coupling surface (*a*) and its two-dimensional projection (*b*) of $^{3}J_{Se,H}$ of diethyl selenide with respect to the internal rotations about the carbon–carbon and carbon–selenium bonds calculated at the SOPPA level. Reproduced from Rusakov and Krivdin [108] with the permission of *John Wiley and Sons*.

Structures 81–89



R = Me (**81**), Et (**82**), Pr^{n} (**83**), Bu^{i} (**84**), Bu^{s} (**85**), cyclo-Hex (**86**), Ph (**87**), CH_2CH_2OH (**88**), CH_2COOH (**89**)

stereochemical studies of a wide range of organoselenium compounds.

A second illustrative example deals with the determination of the stereochemical structures of nine *Z*-2-(vinylsulfanyl)ethenylselanyl organyl sulfides (**81**–**89**) performed by means of the experimental measurements and SOPPA calculations of their ^{77}Se–^{1}H spin–spin coupling constants together with a theoretical conformational analysis performed at the MP2/6-311G(d,p) level.[109] All nine compounds were shown to adopt the preferable skewed *s-cis* conformation of their terminal vinylsulfanyl group, whereas the favourable rotational conformations with respect to the internal rotations about the C–S and C–Se bonds of the ethenyl group were found to be both skewed *s-trans*. Principal contributions defining stereospecificity of geminal and vicinal selenium–hydrogen coupling constants in this series were established to be those arising from the molecular orbitals of the selenium lone pair the and selenium–carbon and carbon–hydrogen chemical bonds, as shown in Fig. 10.

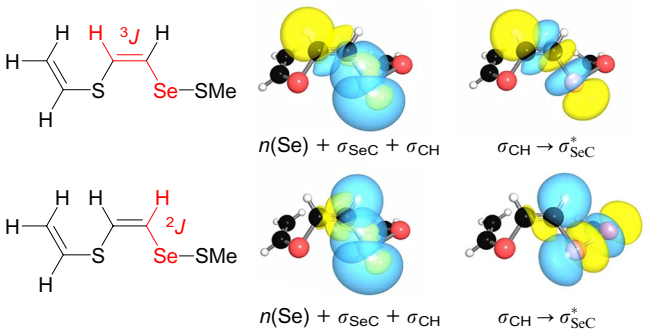


Figure 10. Principal contributions to $^{2}J_{Se,H}$ and $^{3}J_{Se,H}$ in compound **81** adopting a favourable conformation. Reproduced from Rusakov *et al.*[109] with the permission of *John Wiley and Sons*.

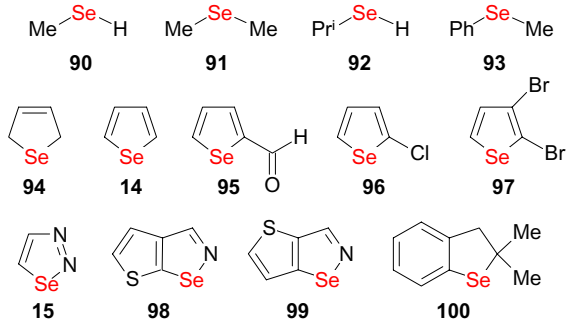
3.2. ^{77}Se–^{13}C spin–spin coupling constants

Very limited data are available on the computation of selenium–carbon spin–spin coupling constants at the modern levels of theory. Herewith, the focus is on the two most representative publications where such calculations were performed at the non-relativistic SOPPA(CC2) level in combination with the fully relativistic four-component method for a series of representative organoselenium compounds.

In the first paper,[110] the four-component fully relativistic calculations of the selenium–carbon spin–spin coupling constants were performed in a series of selenium heterocycles and their parent open-chain precursors **14**, **15**, **90**–**100**, as compared to the non-relativistic most accurate SOPPA(CC2) results.

It was found that full relativistic corrections evaluated at the four-component DFT level were indeed important for the one-bond ^{77}Se–^{13}C couplings contributing to about as

Structures 90–100



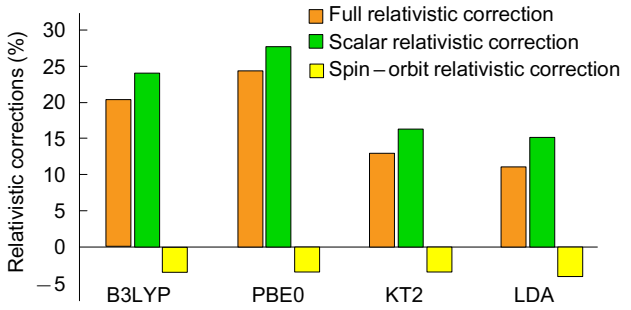


Figure 11. Relativistic corrections to the total values of $^1J_{Se,C}$ calculated in the series of **14**, **15**, **90**–**100** at the four-component DFT level using different functionals. The following functionals have been used: B3LYP (Becke three-parametre hybrid functional in combination with the Lee–Yang-Parr correlation functional), PBE0 (Perdew-Burke-Ernzerhof generalized gradient functional with a predetermined amount of exact exchange), KT2 (generalized gradient exchange-correlation functional of Keal and Tozer) and LDA (local density approximation). *R* is Pearson correlation coefficient. Reproduced from Rusakov *et al.*[110] with the permission of *John Wiley and Sons*.

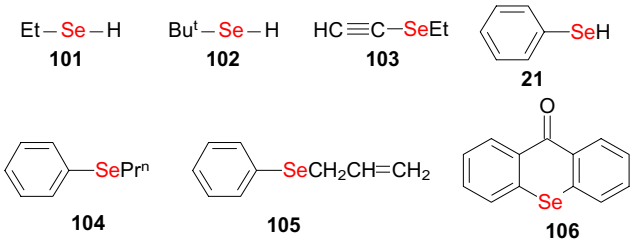
much as 15%–25% of their full relativistic values, depending on the functional. Thus, the B3LYP and PBE0 functionals gave essentially larger full relativistic corrections than those calculated with the KT2 and LDA functionals. In general, relativistic effects were found to be of major importance in the coupling mechanism of the one-bond selenium–carbon couplings, $^1J_{Se,C}$. Scalar and spin–orbit relativistic corrections were calculated based on the full and spin-free relativistic Dirac–Coulomb and non-relativistic Levy–Leblond Hamiltonians using four dedicated DFT functionals. It followed that all scalar corrections were negative dominating positive spin–orbit relativistic corrections. Relative importance of full, scalar and spin–orbit relativistic corrections are shown in Fig. 11.

It was found that negative scalar relativistic corrections increased the total value of $^1J_{Se,C}$ by *ca.* 20% in magnitude while positive spin–orbit relativistic corrections decreased it by about 5%. This result was in line with the fact that scalar relativistic effects deal mainly with the contraction of *s*-orbitals, which are of prime importance in the transmission of the spin–spin coupling mechanism. Solvent effects in the values of $^1J_{Se,C}$, calculated within the polarizable continuum model for the solvents with a broad scope of dielectric constants, were found to be next to negligible decreasing negative $^1J_{Se,C}$ in magnitude by only about 1 Hz.

Based on these results, a combination of the non-relativistic second-order polarization propagator approach with the four-component relativistic density functional theory scheme was recommended as a versatile tool for the calculation of $^1J_{Se,C}$.[110]

In the second paper,[111] a systematic theoretical study of geminal and vicinal $^{77}Se-^{13}C$ spin–spin coupling constants was performed in the series of open-chain selenides and selenium-containing heterocycles **21**, **101**–**106** together with

Structures 21, 101–106



the previously studied unsubstituted selenophene (**14**) and 2,2-dimethyl-2,3-dihydrobenzo[*b*]selenophene (**100**). The main finding of this study was that relativistic effects play an essential role in the selenium–carbon coupling mechanism, especially when the coupling pathway includes a triple bond, contributing to as much as 10%–15% of their total values and noticeably improving the agreement between the calculated couplings and the experiment, as illustrated in Fig. 12. Both geminal and vicinal selenium–carbon coupling constants showed marked stereochemical behaviour, as was exemplified by the calculated dihedral angle dependences with and without taking into account relativistic effects, as shown in Fig. 13. It was concluded[111] that

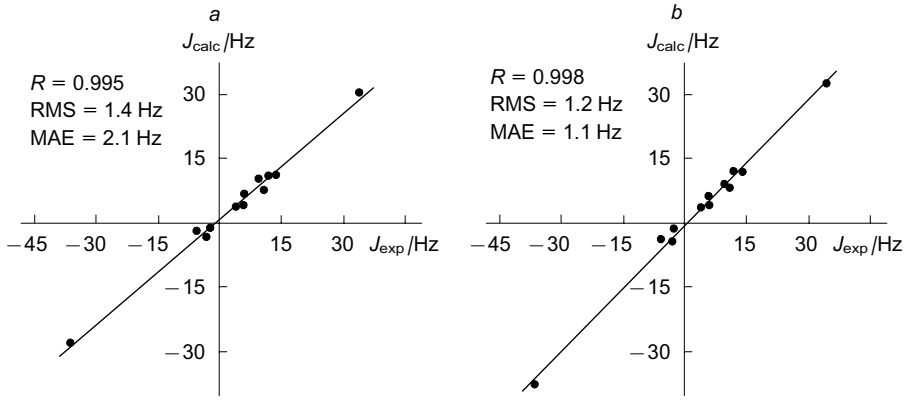


Figure 12. Correlation plots of the conformationally averaged $^2J_{Se,C}$ and $^3J_{Se,C}$ calculated in the series of **14**, **21**, **100**, **101**–**106** at the SOPPA(CC2) level *vs.* experiment: (*a*) without relativistic corrections; (*b*) taking into account relativistic corrections. *R* is Pearson correlation coefficient. Reproduced from Rusakov and Krivdin[111] with the permission of *John Wiley and Sons*.

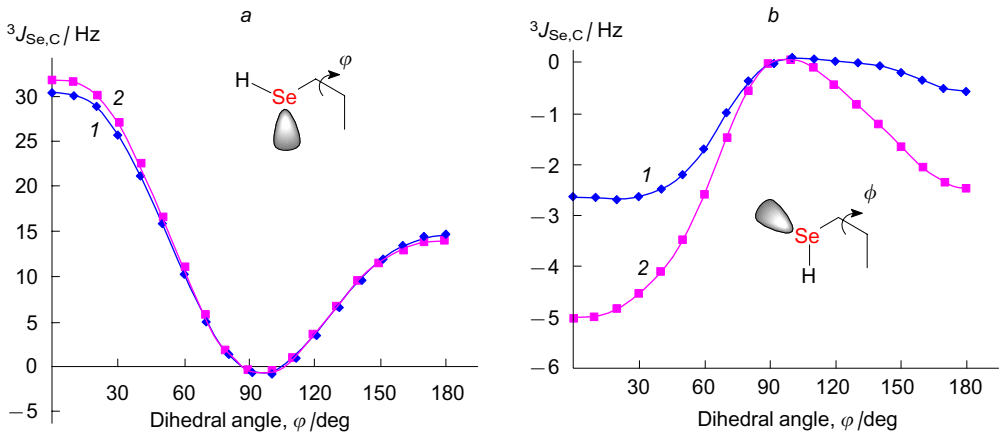


Figure 13. Dihedral angle dependences of $^2J_{Se,C}$ and $^3J_{Se,C}$ in the model propaneselenol adopting *transoidal* (*a*) and *cisoidal* (*b*) conformations, calculated at the SOPPA(CC2) level (*1*) and those with relativistic corrections taken into account (*2*). Reproduced from Rusakov and Krivdin[111] with the permission of *John Wiley and Sons*.

relativistic effects in the $^{77}Se-^{13}C$ spin–spin coupling constants are of prime importance, and that established dependences can be used as a practical guide in stereochemical studies of a broad range of organoselenium compounds.

3.3. $^{77}Se-^{77}Se$ spin–spin coupling constants

Very limited data are available on theoretical calculations of this particular type of coupling constants with the exception of these dealing with the computation of $^1J_{Se,Se}$ in dimethyl diselenide. Among the most illustrative examples of those studies, is the early paper by Tanioku *et al.*[112] where this coupling constant was thoroughly analyzed by employing the triple-zeta Slater-type basis sets at the DFT level. It was found that $^1J_{Se,Se}$ provided marked torsional angular dependence on the rotation about the selenium–selenium bond, as illustrated in Fig. 14. It is seen that stereochemical behaviour of the selenium–selenium coupling constant is mainly determined by the contribution of paramagnetic spin–orbit term, while the dihedral angle dependence of the Fermi contact term is much less pronounced. The reported theoretical dependence of $^1J_{Se,Se}$ also explained the large experimental values of the coupling ranging from 330 to 380 Hz in naphtho[1,8-*cd*][1,2]diselenole (**107**) and its functional derivatives **108**–**113**.

In a more recent paper,[113] the dihedral angle dependence of $^1J_{Se,Se}$ in dimethyl diselenide was reinvestigated in term of the high-level SOPPA(CCSD) method taking into account relativistic effects at the DFT level. The calculated curves are shown in Fig. 15. It is seen that $^1J_{Se,Se}$ demonstrates a pronounced Karplus-type dependence, which is characterized by two maxima at $\varphi = 0$ and 180° and a deep minimum at $\varphi = 90°$. Two curves in Fig. 15 calculated at

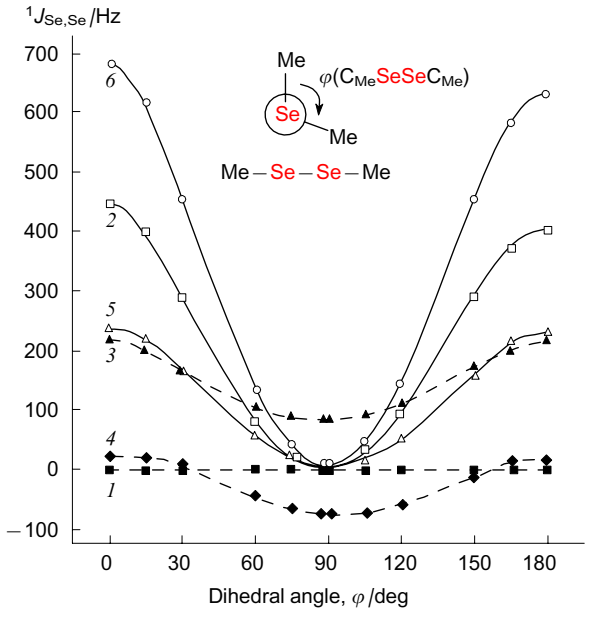
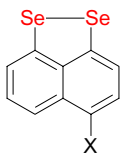


Figure 14. Dihedral angle dependences of the diamagnetic spin–orbit (*1*), paramagnetic spin–orbit (*2*), spin dipolar (*3*), Fermi contact (*4*) and the sum of spin dipolar and Fermi contact (*5*) contributions, together with the total value of the selenium–selenium coupling constant (*6*) of dimethyl diselenide. Reproduced from Tanioku *et al.*[112] under the *Creative Commons Attribution License*.

Structures 107–113



X = H (**107**), Me (**108**), CO_2Me (**109**), CN (**110**), OMe (**111**), NO_2 (**112**), Cl (**113**)

107–113

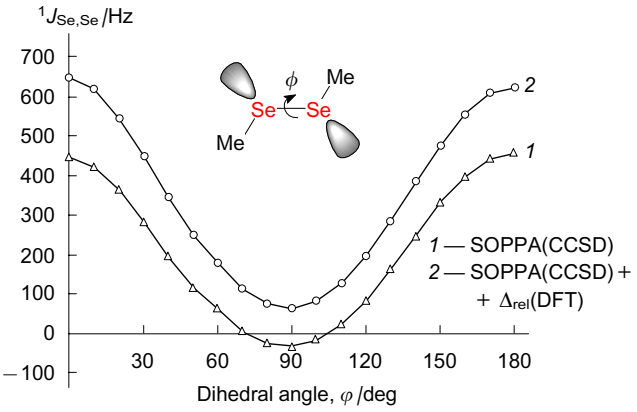


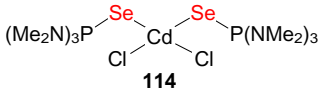
Figure 15. Dihedral angle dependence of $^1J_{Se,Se}$ in dimethyl diselenide calculated at the non-relativistic SOPPA(CCSD) level (*1*) and that with taking into account the relativistic correction at the DFT level (*2*). The value of $\varphi = 0°$ is adopted for the *synperiplanar* orientation. Reproduced from Rusakova *et al.*[113] with the permission of *John Wiley and Sons*.

the non-relativistic and 'relativistically corrected' SOPPA(CCSD) levels look very much the same with the latter shifted upwards by about 150 Hz due to the relativistic correction in each particular point of the dihedral angle scale. The span of $^{1}J_{Se,Se}$ in the range of $\Delta\varphi = 0-90^{\circ}$ (the same for $\Delta\varphi = 90-180^{\circ}$) amounts to as much as almost 600 Hz providing a powerful tool for the stereochemical analysis of a broad range of organoselenium compounds.

3.4. Other coupling constants involving ^{77}Se nucleus

This section is illustrated by the state-of-the art calculations of the one-bond $^{1}J_{Se,P}$ coupling constant in the selenium-containing complex of cadmium, $CdCl_2[(Me_2N)_3PSe]_2$ (**114**), performed in the most recent study by dos Reis Lino *et al.*[114] in search for a computational design strategy for the prescreening of the prospective quantum computers by applying transition metal complexes. Two- and four-component relativistic methods with using the PBE0 functional in combination with the triple-zeta TZ2P and TZ2P-J and quadruple-zeta QZ2P and QZ2P-J basis sets were employed for this purpose.

Structure 114



114

The biggest change in the selenium–phosphorus coupling was observed on going from the TZ2P to the specialized coupling constant basis set TZ2P-J, on which $^{1}J_{Se,P}$ was changed by about 145 Hz. A slightly smaller change was observed on going from the TZ2P to the QZ4P basis set (109 Hz). This implied that the QZ4P basis set should include some of the functions, which are important for the calculation of coupling constants and which are missing in the TZ2P basis set. When moving then from the QZ4P to the corresponding coupling constant basis set QZ4P-J, the further change was found to be even smaller (44 Hz). Finally, the difference between TZ2P-J and QZ4P-J was very small, almost next to negligible, if compared to the total value of this coupling constant (8.9 Hz). So, the main result of the performed study[114] was that the TZ2P-J basis set in combination with the PBE0 exchange-correlation functional used at the two- and four-component relativistic levels appeared to be the optimal choice for the calculation of $^{1}J_{Se,P}$ in the related complexes.

Several years earlier, Rusakova *et al.*[113] performed a systematic study of relativistic effects in the spin–spin coupling constants involving selenium, namely, ^{77}Se–^{15}N, ^{77}Se–^{19}F, ^{77}Se–^{29}Si and ^{77}Se–^{31}P, together with ^{77}Se–^{1}H, ^{77}Se–^{13}C and ^{77}Se–^{77}Se, which are discussed earlier and are not considered in this section. The couplings calculated at the non-relativistic SOPPA(CCSD) level in the series of **115**–**125** extracted from that publication are compiled in Table 4.

Based on these data, it was found that the FC term by far dominated over the sum of all non-contact contributions and was of the same sign as the total values of the coupling constants. Basically, individual contributions of the PSO, DSO and SD terms were small (< 10%), and the contribution of the DSO term was next to negligible (< 0.1%) for all types of coupling constants, which is illustrated in Fig. 16.

At that, relativistic corrections were found to play a major role in the total values of $^{1}J_{Se,X}$, X = N, F, Si and P, reaching as much as 20%, as can be seen in Fig. 17. Scalar relativistic effects (Darwin term together with mass-velocity corrections) by far dominated over the spin–orbit coupling in the total relativistic effects for all $^{1}J_{Se,X}$. Electron correlation effects, not taken into account at the RPA level but evaluated in an inexplicit way in the DFT calculations, do not have major importance in the manifestation

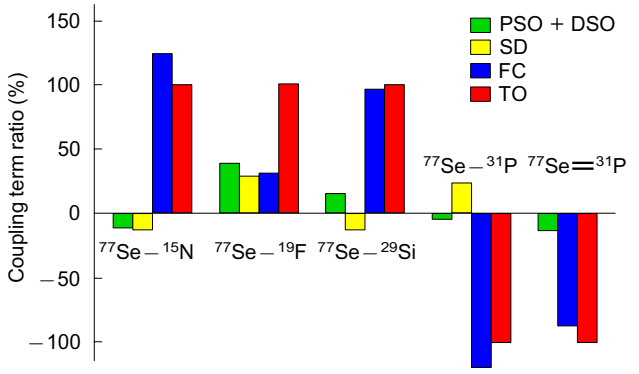


Figure 16. Coupling term ratio of the coupling constants $^{1}J_{Se,X}$, X = N, F, Si, P, calculated at the SOPPA(CCSD) level. Reproduced with minor editing privilege from Rusakova *et al.*[113] with the permission of *John Wiley and Sons*.

Table 4. Typical examples of spin–spin coupling constants $^{1}J_{Se,X}$ calculated in the series of salient organoselenium compounds at the non-relativistic SOPPA(CCSD) level.[a] Compiled from Rusakova *et al.*[113]

Compound	Formula	Coupling constant	DSO	PSO	SD	FC	TO	Experiment [b]
115	$F_3C-Se-NH_2$	$^{1}J_{Se,N}$	−0.03	−6.65	−7.87	76.94	62.39	(+)60.1
116	Me_2SeF_2	$^{1}J_{Se,F}$	0.29	153.90	115.80	125.28	395.27	(+)634.0
117	SeF_6	$^{1}J_{Se,F}$	0.73	−178.88	55.32	−1237.34	−1360.17	(−)1423.0
118	$F_2Se{=}O$	$^{1}J_{Se,F}$	0.31	−124.31	102.75	−813.22	−834.47	(−)837.0
119	F_2SeO_2	$^{1}J_{Se,F}$	0.47	−139.19	64.64	−1311.84	−1385.92	(−)1580.0
120	$Et-Se-SiMe_3$	$^{1}J_{Se,Si}$	−0.05	11.79	−9.37	70.49	72.86	(+)107.3
121	$Me-Se-PMe_2$	$^{1}J_{Se,P}$	0.08	−10.33	53.08	−265.35	−222.52	(−)205 ± 6
122	$Me-Se-POMe_2$	$^{1}J_{Se,P}$	0.13	−16.96	32.36	−275.33	−259.80	(−)367.9
123	$Me_3P{=}Se$	$^{1}J_{Se,P}$	0.10	−103.56	5.71	−649.30	−747.05	(−)684.0
124	$F_3P{=}Se$	$^{1}J_{Se,P}$	0.17	−118.23	5.14	−1152.87	−1265.79	(−)1490.0
125	$Cl_3P{=}Se$	$^{1}J_{Se,P}$	0.16	−123.01	1.94	−983.67	−1104.58	(−)1065.0

[a] All coupling constants and their contributions are in Hz. [b] Taken from different sources. For references, see the original paper.[113] Signs (in parenthesis) are assigned based on the performed calculations.

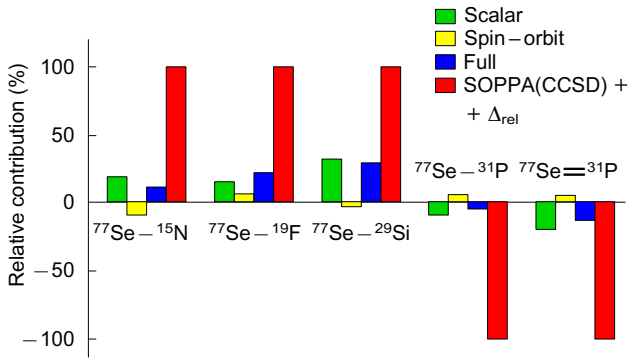


Figure 17. Relative contributions of the scalar, spin–orbit and full relativistic corrections to $^{1}J_{Se,X}$, X = N, F, Si and P, calculated at the RPA level. Reproduced with minor editing privilege from Rusakova *et al.*[113] with the permission of *John Wiley and Sons*.

of relativistic effects in spin–spin couplings involving selenium. Taking into account relativistic corrections essentially improved the agreement between the theoretical results and the experiment demonstrating the importance of relativistic corrections in the calculations of the one-bond spin–spin coupling constants involving selenium, while spin-orbit corrections were found to be rather small throughout the series **115**–**125** (< 10%).[113]

4. Conclusion

Calculations of ^{77}Se NMR chemical shifts and spin–spin coupling constants involving selenium at different levels of theory in the diversity of organoselenium compounds and transition metal complexes with the selenium-containing ligands are rapidly developing and becoming of more and more practical interest. Computation of spin–spin coupling constants involving selenium is much less common, as compared to that of the ^{77}Se NMR chemical shifts. In view of a significant progress in computational NMR, such calculations are on the cutting edge of the modern computational chemistry, and the present review, focusing on the most essential papers in this area of the last decade, seems to be urgent and timely. At that, a vivid progress is also observed in the theoretical interpretation of stereoelectronic effects involving selenium atom, studied based on the calculations of the ^{77}Se NMR parametres, which also claimed for a thorough consideration given in the present review.

Glossary of abbreviations:

B3LYP — Becke three-parametre hybrid functional in combination with the Lee–Yang–Parr correlation functional

CBS — complete basis set,

CC3 — coupled cluster singles, doubles and triples model,

CCSD — coupled cluster single and double excitation model,

CCSD(T) — coupled cluster single and double excitation model with perturbative triples corrections,

COSMO — conductor-like screening model,

DFT — density functional theory,

DMSO — dimethyl sulfoxide,

DSO — diamagnetic spin–orbit (contribution),

FC — Fermi contact (contribution),

GGA — generalized gradient approximation,

GIAO — gauge–including atomic orbitals,

EOM–CCSD — equations-of-motion coupled cluster single and double excitation model,

HF — Hartree–Fock,

IEF-PCM — integral equation formalism polarizable continuum model,

KT2 — generalized gradient exchange-correlation functional of Keal and Tozer,

KT3 — generalized gradient exchange-correlation functional of Keal and Tozer with the gradient-corrected exchange and correlation terms,

LDA — local density approximation,

LDBS — locally dense basis set,

LMO — localized molecular orbital,

LP — lone pair,

LUMO — lowest unoccupied molecular orbital,

MAE — mean absolute error,

MO — molecular orbital,

MP2 — second-order Møller–Plesset perturbation theory,

NBO — natural bond orbital,

NHC — *N*-heterocyclic carbenes,

NMR — nuclear magnetic resonance,

NPA — natural population analysis,

ORTEP — oak ridge thermal ellipsoid plot,

PBE — Perdew–Burke–Ernzerhof generalized gradient functional,

PBE0 — Perdew–Burke–Ernzerhof generalized gradient functional with a predetermined amount of exact exchange,

PCM — polarizable continuum model,

PSO — paramagnetic spin–orbit (contribution),

R — Pearson correlation coefficient,

RHF — restricted Hartree–Fock,

RMS — root mean squares,

RPA — random phase approximation,

SD — spin dipolar (contribution),

SO — spin–orbit,

SOPPA — second-order polarization propagator approach;

SOPPA(MP2) — second-order polarization propagator approach in combination with Møller–Plesset perturbation theory,

SOPPA(CC2) — second-order polarization propagator approach in combination with second-order approximate coupled cluster model,

SOPPA(CCSD) — second-order polarization propagator approach in combination with coupled cluster single and double excitation model,

TO — total (sum of all coupling contributions),

ZORA — zeroth order regular approximation,

ZPVC — zero-point vibrational correction.

References

1. S.P.A.Sauer. *Molecular Electromagnetism. A Computational Chemistry Approach*. (Oxford: University Press, 2012)
2. T.Helgaker, M.Jaszuński, K.Ruud. *Chem. Rev.*, **99**, 293 (1999)
3. T.Helgaker, M.Jaszuński, M.Pecul. *Prog. NMR Spectrosc.*, **53**, 249 (2008)
4. G.A.Aucar, R.H.Romero, A.F.Maldonado. *Int. Rev. Phys. Chem.*, **29**, 1 (2010)
5. *High Resolution NMR Spectroscopy: Understanding Molecules and their Electronic Structures*. (Ed. R.H.Contreras). (The Netherlands: Elsevier, 2013)

6. Y.Y.Rusakov, L.B.Krivdin. *Russ. Chem. Rev*., **82**, 99 (2013)
7. F.A.A.Mulder, M.Filatov. *Chem. Soc. Rev*., **39**, 578 (2010)
8. L.B.Krivdin, R.H.Contreras. *Ann. Rep. NMR Spectrosc*., **61**, 133 (2007)
9. Y.Xiao, W.Liu, J.Autschbach. In *Handbook of Relativistic Quantum Chemistry. Relativistic Theories of NMR Shielding*. (Ed. W.Liu). (Berlin: Springer, 2017)
10. J.Autschbach. *Phyl. Trans. Royal Soc. A*, **372**, 1 (2014)
11. M.Repisky, S.Komorovsky, R.Bast, K.Ruud. In *Gas Phase NMR. Relativistic Calculations of Nuclear Magnetic Resonance Parameters*. (Eds K.Jackowski, M.Jaszunski). (Cambridge: The Royal Society of Chemistry, 2016)
12. I.L.Rusakova, Y.Y.Rusakov, L.B.Krivdin. *Russ. Chem. Rev*., **85**, 356 (2016)
13. L.B.Krivdin. *Magn. Reson. Chem*., **57**, 897 (2019)
14. L.B.Krivdin. *Magn. Reson. Chem*., **58**, 5 (2020)
15. L.B.Krivdin. *Magn. Reson. Chem*., **58**, 15 (2020)
16. L.B.Krivdin. *Prog. NMR Spectrosc*., **108**, 17 (2018)
17. L.B.Krivdin. *Prog. NMR Spectrosc*., **112 – 113**, 103 (2019)
18. L.B.Krivdin. *Prog. NMR Spectrosc*., **102 – 103**, 98 (2017)
19. L.B.Krivdin. *Prog. NMR Spectrosc*., **105**, 54 (2018)
20. L.B.Krivdin. *Russ. Chem. Rev*., **89**, 1040 (2020); https://doi.org/10.1070/RCR4948
21. L.B.Krivdin. *Russ. Chem. Rev*., **89**, 449 (2020); https://doi.org/10.1070/RCR4927
22. L.B.Krivdin. *Magn. Reson. Chem*., **58**, (2020); https://doi.org/10.1002/mrc.4965
23. L.B.Krivdin. *Magn. Reson. Chem*., **58**, (2020); https://doi.org/10.1002/mrc.4973
24. I.L.Rusakova, L.B.Krivdin. *Mendeleev Commun*., **28**, 1 (2018)
25. L.B.Krivdin, Y.Y.Rusakov. *Encycl. Magn. Reson*., **3**, 87 (2014)
26. M.Bühl, J.Gauss, J.F.Stanton. *Chem. Phys. Lett*., **241**, 248 (1995)
27. M.Bühl, W.Thiel, U.Fleischer, W.Kutzelnigg. *J. Phys. Chem*., **99**, 4000 (1995)
28. G.Schreckenbach, Y.Ruiz-Morales, T.Ziegler. *J. Chem. Phys*., **104**, 8605 (1996)
29. G.Balzer, H.Duddeck, U.Fleischer, F.Röhr. *Fresenius J. Anal. Chem*., **357**, 473 (1997)
30. J.Lounila, J.Vaara, Y.Hiltunen, A.Pulkkinen, J.Jokisaari, M.Ala-Korpela. *J. Chem. Phys*., **107**, 1350 (1997)
31. P.J.Wilson. *Mol. Phys*., **99**, 363 (2001)
32. J.Komulainen, R.S.Laitinen, R.J.Suontamo. *Can. J. Chem*., **80**, 1435 (2002)
33. J.Jokisaari, J.Autschbach. *Phys. Chem. Chem. Phys*., **5**, 4551 (2003)
34. C.A.Bayse. *Inorg. Chem*., **43**, 1208 (2004)
35. C.A.Bayse. *J. Chem. Theory Comput*., **1**, 1119 (2005)
36. J.M.Rautiainen, T.Way, G.Schatte, J.Passmore, R.S.Laitinen, R.J.Suontamo, J.Valkonen. *Inorg. Chem*., **44**, 1904 (2005)
37. S.Hayashi, W.Nakanishi. *Bioinorg. Chem. Appl*., **2006**, 1 (2006)
38. W.Nakanishi, S.Hayashi, D.Shimizu, M.Hada. *Chem. – Eur. J*., **12**, 3829 (2006)
39. C.Bayse, S.Antony. *Main Group Chem*., **6**, 185 (2007)
40. W.Nakanishi, S.Hayashi, M.Hada. *Chem. – Eur. J*., **13**, 5282 (2007)
41. B.Wrackmeyer, Z.G.Hernández, M.Herberhold. *Magn. Reson. Chem*., **45**, 198 (2007)
42. A.V.Afonin, D.V.Pavlov, I.A.Ushakov, E.Y.Schmidt, A.I.Mikhaleva. *Magn. Reson. Chem*., **47**, 879 (2009)
43. A.V.Afonin, D.V.Pavlov, A.I.Albanov, E.P.Levanova, G.G.Levkovskaya. *Magn. Reson. Chem*., **49**, 740 (2011)
44. S.Brownridge, L.Calhoun, H.D.B.Jenkins, R.S.Laitinen, M.P.Murchie, J.Passmore, J.Pietikäinen, J.M.Rautiainen, J.C.P.Sanders, G.J.Schrobilgen, R.J.Suontamo, H.M.Tuononen, J.U.Valkonen, C.-M.Wong. *Inorg. Chem*., **48**, 1938 (2009)
45. Y.Y.Rusakov, L.B.Krivdin. *J. Comp. Chem*., **36**, 1756 (2015)
46. Y.Y.Rusakov, I.L.Rusakova, L.B.Krivdin. *Magn. Reson. Chem*., **53**, 485 (2015)
47. J.Liu, Z.Zhang, S.Rozovsky. *FEBS Lett*., **588**, 3311 (2014)
48. C.Fan, J.Chen, Y.Wang, Y.-S.Wong, Y.Zhang, W.Zheng, W.Cao, T.Chen. *Free Radical Biol. Med*., **65**, 305 (2013)
49. C.Fan, W.Zheng, X.Fu, X.Li, Y.-S.Wong, T.Chen. *Oncotarget*, **5**, 2853 (2014)
50. S.L.Balof, B.Yu, A.B Lowe, Y.Ling, Y.Zhang, H.J.Schanz. *Eur. J. Inorg. Chem*., **2009**, 1717 (2009)
51. J.Struppe, Y.Zhang, S.Rozovsky. *J. Phys. Chem. B*, **119**, 3643 (2015)
52. V.Sladek, L.Rottmannová, P.Škora, M.Ilčin, V.Lukeš. *Acta Chim. Slovaca*, **5**, 159 (2012)
53. V.P.Singh, J.Poon, L.Engman. *J. Org. Chem*., **78**, 1478 (2013)
54. V.P.Singh, J.Poon, R.J.Butcher, L.Engman. *Chem. – Eur. J*., **20**, 12563 (2014)
55. V.P.Singh, H.B.Singh, R.J.Butcher. *Eur. J. Org. Chem*., **2011**, 5485 (2011)
56. V.P.Singh, H.B.Singh, R.J.Butcher. *Chem. – Asian J*., **6**, 1431 (2011)
57. S.Kumar, J.Yan, J.Poon, V.P.Singh, X.Lu, M.K.Ott, L.Engman, S.Kumar. *Angew. Chem., Int. Ed*., **55**, 3729 (2016)
58. V.P.Singh, J.-F.Poon, R.J.Butcher, X.Lu, G.Mestres, M.K.Ott, L. Engman. *J. Org. Chem*., **80**, 7385 (2015)
59. V.P.Singh, J.-F.Poon, J.Yan, X.Lu, M.K.Ott, R.J.Butcher, P.J.Gates, L.Engman. *J. Org. Chem*., **82**, 313 (2017)
60. M.Zielińska-Błajet, P J.Boratyński, J.Palus, J.Skarzewski. *Tetrahedron*, **69**, 10223 (2013)
61. A.D.Becke. *J. Chem. Phys*., **109**, 2092 (1998)
62. P.J.Wilson, T.J.Bradley, D.J.Tozer. *J. Chem. Phys*., **115**, 9233 (2001)
63. K.A.Chernyshev, L.B.Krivdin, S.V.Fedorov, S.N.Arbuzova, N.I.Ivanova. *Russ. J. Org. Chem*., **49**, 1420 (2013)
64. H.Clavier, S.P.Nolan. *Chem. Commun*., **46**, 841 (2010)
65. A.Poater, B.Cosenza, A.Correa, S.Giudice, F.Ragone, V.Scarano, L.Cavallo. *Eur. J. Inorg. Chem*., **2009**, 1759 (2009)
66. D.J.Nelson, S.P.Nolan. *Chem. Soc. Rev*., **42**, 6723 (2013)
67. H.Jacobsen, A.Correa, C.Costabile, L.Cavallo. *J. Organomet. Chem*., **691**, 4350 (2006)
68. H.Jacobsen, A.Correa, A.Poater, C.Costabile, L.Cavallo. *Coord. Chem. Rev*., **253**, 687 (2009)
69. S.Fantasia, J.L.Petersen, H.Jacobsen, L.Cavallo, S.P.Nolan. *Organometallics*, **26**, 5880 (2007)
70. D.J.Nelson, A.Collado, S.Manzini, S.Meiries, A.M.Z.Slawin, D.B.Cordes, S.P.Nolan. *Organometallics*, **33**, 2048 (2014)
71. O.Santoro, A.Collado, A.M.Z.Slawin, S.P.Nolan, C.S.J.Cazin. *Chem. Commun*., **49**, 10483 (2013)
72. F.Ragone, A.Poater, L.Cavallo. *J. Am. Chem. Soc*., **132**, 4249 (2010)
73. S.V.C. Vummaleti, D.J.Nelson, A.Poater, A.Gómez-Suárez, D.B.Cordes, A.M.Z.Slawin, S.P.Nolan, L.Cavallo. *Chem. Sci*., **6**, 1895 (2015)
74. A.Liske, K.Verlinden, H.Buhl, K.Schaper, C.Ganter. *Organometallics*, **32**, 5269 (2013)
75. K.Verlinden, H.Buhl, W.Frank, C.Ganter. *Eur. J. Inorg. Chem*., **2015**, 2416 (2015)
76. T.J.Emge, M.D.Romanelli, B.F.Moore, J.G.Brennan. *Inorg. Chem*., **49**, 7304 (2010)
77. K.Norton, S.Banerjee, S.Das, L.Huebner, T.J.Emge, J.G.Brennan. *Dalton Trans*., **39**, 6794 (2010)
78. A.Kornienko, B.F.Moore, G.A.Kumar, M.-C.Tan, R.E.Riman, M.G.Brik, T.J.Emge, J.G.Brennan. *Inorg. Chem*., **50**, 9184 (2011)
79. B.F.Moore, G.A.Kumar, M.-C.Tan, J.Kohl, R.E.Riman, M.G.Brik, T.J.Emge, J.G.Brennan. *J. Am. Chem. Soc*., **133**, 373 (2011)
80. B.F.Moore, T.J.Emge, J.G.Brennan. *Inorg. Chem*., **52**, 6021 (2013)

81. K.Holligan, P.Rogler, D.Rehe, M.Pamula, A.Y.Kornienko, T.J.Emge, K.Krogh-Jespersen, J.G.Brennan. *Inorg. Chem.*, **54**, 8896 (2015)
82. D.Rehe, A.Y.Kornienko, T.J.Emge, J.G.Brennan. *Inorg. Chem.*, **55**, 6961 (2016)
83. M.A.Stuber, A.Y.Kornienko, T.J.Emge, J.G.Brennan. *Inorg. Chem.*, **56**, 10247 (2017)
84. M.Ringgold, W.Wu, M.Stuber, A.Y.Kornienko, T.J.Emge, J.G.Brennan. *Dalton Trans.*, **47**, 14652 (2018)
85. M.Ringgold, D.Rehe, P.Hrobárik, A.Y.Kornienko, T.J.Emge, J.G.Brennan. *Inorg. Chem.*, **57**, 7129 (2018)
86. W.Wu, X.Zhang, A.Y.Kornienko, G.A.Kumar, D.Yu, T.J.Emge, R.E.Riman, J.G.Brennan. *Inorg. Chem.*, **57**, 1912 (2018)
87. W.Wu, D.Rehe, P.Hrobárik, A.Y.Kornienko, T.J.Emge, J.G.Brennan. *Inorg. Chem.*, **57**, 14821 (2018)
88. M.M.Karjalainen, R.Oilunkaniemi, R.S.Laitinen. *Inorg. Chim. Acta*, **390**, 79 (2012)
89. A.J.Karhu, M.Risto, J.M.Rautiainen, R.Oilunkaniemi, T.Chivers, R.S.Laitinen. *Can. J. Chem.*, **94**, 342 (2016)
90. A.J.Karhu, O.J.Pakkanen, J.M.Rautiainen, R.Oilunkaniemi, T.Chivers, R.S.Laitinen. *Inorg. Chem.*, **54**, 4990 (2015)
91. M.M.Karjalainen, W.Weigand, R.Oilunkaniemi, R.S.Laitinen. *Polyhedron*, **101**, 244 (2015)
92. E.M.Takaluoma, T.T.Takaluoma, R.Oilunkaniemi, R.S.Laitinen. *Z. Anorg. Allg. Chem.*, **641**, 772 (2015)
93. A.J.Karhu, O.J.Pakkanen, J.M.Rautiainen, R.Oilunkaniemi, T.Chivers, R.S.Laitinen. *Dalton Trans.*, **45**, 6210 (2016)
94. M.M.Karjalainen, C.Sanchez-Perez, J.M.Rautiainen, R.Oilunkaniemi, R.S.Laitinen. *CrystEngComm*, **18**, 4538 (2016)
95. A.J.Karhu, J.Jämsä, J.M.Rautiainen, R.Oilunkaniemi, T.Chivers, R.S.Laitinen. *Z. Anorg. Allg. Chem.*, **643**, 495 (2017)
96. C.Sanchez-Perez, C.E.Knapp, M.M.Karjalainen, R.Oilunkaniemi, C.J.Carmalt, R.S.Laitinen. *Dalton Trans.*, **47**, 5415 (2018)
97. H.Laasonen, J.Ikäheimonen, M.Suomela, J.M.Rautiainen, R.S.Laitinen. *Molecules*, **24**, 319 (2019)
98. G.Schreckenbach, Y.Ruiz-Morales, T.Ziegler. *J. Chem. Phys.*, **104**, 8605 (1996)
99. M.Bühl, W.Thiel, U.Fleischer, W.Kutzelnigg. *J. Phys. Chem.*, **99**, 4000 (1995)
100. Y.Y.Rusakov, L.B.Krivdin, N.V.Istomina, V.A.Potapov, S.V.Amosova. *Magn. Reson. Chem.*, **46**, 979 (2008)
101. Y.Y.Rusakov, L.B.Krivdin, N.V.Istomina, E.P.Levanova, G.G.Levkovskaya. *Aust. J. Chem.*, **62**, 734 (2009)
102. Y.Y.Rusakov, L.B.Krivdin, S.P.A.Sauer, E.P.Levanova, G.G.Levkovskaya. *Magn. Reson. Chem.*, **48**, 44 (2010)
103. K.E.Kövér, A.A.Kumar, Y.Y.Rusakov, L.B.Krivdin, T.-Z.Illyés, L.Szilágyi. *Magn. Reson. Chem.*, **49**, 190 (2011)
104. Y.Y.Rusakov, L.B.Krivdin, V.A.Potapov, M.V.Penzik, S.V.Amosova. *Magn. Reson. Chem.*, **49**, 389 (2011)
105. Y.Y.Rusakov, L.B.Krivdin, N.V.Orlov, V.P.Ananikov. *Magn. Reson. Chem.*, **49**, 570 (2011)
106. Y.Y.Rusakov, L.B.Krivdin, A.A.Kumar, L.Szilágyi, K.E.Kövér. *Magn. Reson. Chem.*, **50**, 488 (2012)
107. Y.Y.Rusakov, L.B.Krivdin, L.K.Papernaya, A.A.Shatrova. *Magn. Reson. Chem.*, **50**, 169 (2012)
108. Y.Y.Rusakov, L.B.Krivdin. *Magn. Reson. Chem.*, **50**, 557 (2012)
109. Y.Y.Rusakov, L.B.Krivdin, M.V.Penzik, V.A.Potapov, S.V.Amosova. *Magn. Reson. Chem.*, **50**, 653 (2012)
110. Y.Y.Rusakov, I.L.Rusakova, L.B.Krivdin. *Magn. Reson. Chem.*, **52**, 214 (2014)
111. Y.Y.Rusakov, L.B.Krivdin. *Magn. Reson. Chem.*, **53**, 93 (2014)
112. A.Tanioku, S.Hayashi, W.Nakanishi. *Bioinorg. Chem. Appl.*, **2009**, 381925 (2009)
113. I.L.Rusakova, Y.Y.Rusakov, L.B.Krivdin. *Magn. Reson. Chem.*, **52**, 500 (2014)
114. J.B.R.Lino, S.P.A.Sauer, T.C.Ramalho. *J. Phys. Chem. C*, **124**, 4946 (2020)